

2D-3D Vortex Line Transition in Two-Layer Josephson Arrays

Wenbin Yu and D. Stroud

Department of Physics, The Ohio State University, Columbus, OH 43210

(November 29, 2018)

Abstract

We calculate the dynamical response of two-layer Josephson arrays to a bias current applied into only one layer (primary layer), in a perpendicular magnetic field. The pancake vortices in the two layers sometimes form into flux lines which move as a unit under the influence of the bias current. The lines break apart into independent pancakes in sufficiently high currents, sufficiently weak interlayer coupling, or possibly sufficiently high fields. We discuss the relevance of these results to recent experiments in high- T_c superconductors in the flux transformer geometry.

PACS numbers: 74.50.+r, 74.60.Ge, 74.60.Jg, 74.70.Mq

I. INTRODUCTION

The so-called “flux-transformer” geometry [1,2]. provides a novel way to study vortex order in Type-II superconductors. In this technique, the external current density \mathbf{J} is injected into and parallel to the upper ab plane of a high- T_c superconductor. The voltage drop is measured across both the upper plane (the “primary voltage”) and the lower plane (the “secondary voltage”). For applied magnetic field $\mathbf{B}\parallel c$, the geometry is sensitive to the vortex order, especially to the interlayer coupling between the so-called vortex “pancakes” in the 2D layers. Typically, this coupling will cause the pancakes to form into flux lines. The $\mathbf{J} \times \mathbf{B}$ Magnus force will exert a torque on such a flux line. If the interlayer coupling is strong enough, the flux line will move as a unit under this force, producing equal primary and secondary voltages. But at sufficiently large \mathbf{J} , for any large anisotropy, the influence of the torque will exceed that of the interlayer coupling, and the flux line will break. Even at small applied currents, the flux line can sometimes be broken by thermal noise. In both cases, the line breaking shows up in the difference between the primary and the secondary voltages, which increases quickly from zero as the pancakes decouple.) This cross-over from 3D flux lines to 2D vortex pancakes has attracted great experimental and theoretical interest [3–11].

In this paper, rather than treating the actual high- T_c superconductor directly, we model the $T = 0$ flux line dynamics in the flux-transformer geometry, using a two-layer Josephson junction array. While far from a realistic high- T_c material, this model is numerically tractable [12,13], and in addition could be directly studied experimentally. We find that in this flux-transformer geometry, the vortex lines do exhibit a 3D-2D decoupling transition at a critical vortex velocity, just as in the high- T_c materials. We map out this transition as a function of anisotropy and applied current, and find behavior which qualitatively resembles experiment. Our calculations show that this transition can be caused by Josephson coupling alone, without other types of interactions (e. g., electromagnetic interactions [1,2], Coulomb interactions [14]) between the pancakes on different layers.

II. MODEL

We consider a two-layer square arrangements of Josephson junctions (cf. Fig. 1). All the junctions, both within and between the planes, are assumed to be overdamped, resistively shunted junctions (RSJ model). All intralayer and interlayer junctions are assumed identical, with critical currents and resistances I_c, R and I_c', R respectively. The ratio $\alpha \equiv I_c'/I_c$ represents the array anisotropy, and is the analog of the high- T_c mass anisotropy.

To simulate the flux-transformer geometry, we inject a bias current along the y direction into only the upper layer (the “primary” layer; cf. Fig. 1) [9]. We denote the other the *secondary* layer. To introduce vortices, we apply a magnetic field $\mathbf{B} \parallel z$, i. e., perpendicular to the layers. The Magnus ($\mathbf{J} \times \mathbf{B}$) force from the transport current will drive these vortices in the x direction.

The equations of motion for this system take the standard form $I_{ij} = V_{ij}/R_{ij} + I_{c;ij} \sin(\phi_i - \phi_j - A_{ij})$, $V_{ij} \equiv V_i - V_j = (\hbar/2e)(d/dt)(\phi_i - \phi_j)$, and $\sum_j I_{ij} = I_{i;ext}$. Here I_{ij} is the total current from grain i to grain j ; R_{ij} and $I_{c;ij}$ are the shunt resistance and critical current of the Josephson coupling between grain i and grain j ; ϕ_i is the phase of the order parameter on grain i ; and $I_{i;ext}$ is the external current fed into grain i . V_{ij} and A_{ij} are the voltage difference and magnetic gauge phase factor between grain i and grain j . $A_{ij} = (2\pi/\Phi_0) \int_{\mathbf{x}_i}^{\mathbf{x}_j} \mathbf{A} \cdot d\mathbf{l}$, where $\Phi_0 \equiv hc/(2e)$ is the flux quantum, \mathbf{A} is the vector potential for the applied magnetic field and \mathbf{x}_i is the position of the center of grain i . The first equation describes the total current between grains i and j as the sum of two terms: an Ohmic current through the shunt resistance, and a Josephson current. The second is Josephson equation relating voltage and phase, while the last is just Kirchhoff’s Law, describing current conservation at the i^{th} node.

As boundary conditions, we introduce a uniform current $I_{i;ext} = I$ into each boundary grain in the primary layer and extract it from the other edge (cf. Fig. 1). In the secondary layer, we use free boundary conditions in the y direction. In both layers, periodic boundary conditions are adopted in the x direction. $A_{ij} = 0$ for an interplanar junction, while for an

intraplanar junction $\sum_{\text{plaquette}} A_{ij} = 2\pi \frac{BS}{\Phi_0} \equiv 2\pi f$ (S is the plaquette area) [15]. We consider only $f = 1/N^2$ so that there is only one vortex (i. e. one flux quantum) piercing each layer. We denote these the primary and secondary vortices.

We solve the coupled equations of motion as described previously [15], using a fourth-order Runge-Kutta algorithm. During the calculation of the dynamical state $\{\phi_i(t)\}$, we keep track of the vortex motion in the array, in terms of the vortex number n of each plaquette. n is defined by $\sum_{\text{plaquette}} (\phi_i - \phi_j - A_{ij}) + 2\pi f = 2\pi n$, where $(\phi_i - \phi_j - A_{ij})$ is in the range $(-\pi, \pi]$ and the summation is taken in the counterclockwise direction.

III. $I - \langle V \rangle$ CHARACTERISTICS

Our $I - \langle V \rangle$ characteristics typically fall into one of five regimes. (i) At the lowest currents, $\langle V \rangle = 0$: both primary and secondary vortices are pinned by the periodic potential of the array [16,17]. (ii) At slightly higher currents, in some cases, the primary vortices move, while the secondary vortices are still pinned. (iii) In other arrays, at such currents, both primary and secondary vortices are depinned and move together as a single flux line. (iv) At still higher currents, in some arrays, both vortices are depinned, but move *independently*, as separate “pancakes”. (v) For $I > I_c$, the entire Josephson lattice is depinned, and the $I - \langle V \rangle$ characteristics are dominated by single-junction effects.

Fig. 2 shows the calculated $I - \langle V \rangle$ characteristics of a $2 \times 10 \times 10$ ($N = 10$) array at $f = 0.01$ and three values of α . In the flux-flow regime [cases (ii)-(iv)], the $I - \langle V \rangle$ curves are dominated by vortex motion. In all cases, whether moving or fixed, these vortices remain in the center of the array (i. e. the 5th row), presumably the region of lowest energy. (In our 19×19 array calculations, they stay in the 10th row.)

The critical current for the onset of voltage is very sensitive to the anisotropy α . When $\alpha = 0$, Fig. 2(b) shows that the primary vortex is depinned at the bias current $I_{cp} \approx 0.1I_c$, while the secondary vortex remains fixed up to a bias current $I_{cs} \approx 0.28I_c$. At $\alpha = 0.01$, these depinning currents are respectively $0.16I_c$ and $0.26I_c$. But when $\alpha = 0.04$, the primary

and the secondary vortices are depinned *simultaneously* near $0.17I_c$, and move thereafter as a single flux line in the array. This line, however, breaks apart near $I_{cd} = 0.36I_c$, above which the primary vortex moves faster than the secondary vortex. For all three α values, the individual junctions in the primary layer go normal near $I_{cj} = 1.06I_c$.

In the zero-coupling limit, the value $I_{cp} = 0.1I_c$ [cf. Fig. 2(b)] is the depinning current of a single vortex in a 2D array [16]. This can be understood by the following argument. Below I_{cp} , there is zero voltage drop across every junction. Hence, no current passes through the resistive shunts between layers. Moreover, since $\alpha = 0$, there is no interlayer Josephson current. Therefore, all the bias current passes only through the primary layer, and I_{cp} must be the vortex depinning current for a single-layer array. Once the primary vortex has been depinned, there is some voltage drop between the layers. This voltage drop produces currents into the secondary layer via the interlayer shunt resistances. For sufficiently large I , these currents generate a Magnus force which depins the secondary vortex.

At sufficiently small *nonzero* α , we still find that $I_{cp} < I_{cs}$. But above a critical α_c , $I_{cp} = I_{cs}$, and the two vortices move together as a single flux line for $I > I_{cp}$. α_c seems also to be size-dependent.

We can crudely understand all of these phenomena from a simple argument. The idea is illustrated schematically in Fig. 3, which shows a side view of an $N = 11$ array with transport current injected from the left. The primary and secondary vortices – both located in the middle row of the array – are indicated by crosses. Since the vertical junctions have critical current αI_c , the total current passing through these junctions into the secondary layer, under zero voltage conditions, cannot exceed $\approx \frac{1}{2}\alpha NI_c$ to the left of the vortex. Assume that the transport current injected into the primary layer will divide equally between the two layers until this limit is exceeded. This occurs at a transport current $I_{eq} = \alpha NI_c$. From this picture, we can estimate the conditions on N and α such that the two vortices will be depinned *simultaneously*. Namely, if $N\alpha/2 > 0.1$, then *both* vortices will be depinned simultaneously at current below this limiting current and move together thereafter under the bias current drive. Conversely, if $N\alpha/2 \leq 0.1$, the vortices will be depinned at different

currents, and will move more or less independently. (Note that if there were no resistive shunt coupling between layers, then at $\alpha = 0$ value, the two layers would be entirely independent the secondary vortex would never be depinned.)

For $N = 10$, the above argument gives $0.02 < \alpha_c < 0.03$, consistent with our numerical results. For an $N = 19$ array, the corresponding value of α_c , both analytically and numerically, is in the range $0.01 < \alpha_c < 0.02$. To test this picture further, we have also calculated the current distribution in the array for a variety of parameters. The distribution of currents in the vertical junctions indeed conforms with the estimates given above.

This picture may possibly explain the breaking of the flux line at large enough I . As I increases, the line moves faster and faster, but the secondary vortex will lag the primary one by an increasing distance. Eventually, this distance may be such that (in a small array) the secondary vortex will start to feel the influence of the *images* of the primary vortex. Above this current, the primary and secondary vortices should break apart and move separately.

These arguments suggest two conclusions. First, for large enough N , the primary and the secondary vortex will *always* form a single flux line – that is, will be depinned and move together – for an arbitrarily weak but nonzero interlayer Josephson coupling α . Secondly, in a sufficiently large array, the line should remain unbroken all the way up to the single-junction critical current I_c [18]. We have carried out a few calculations for larger arrays, which do support these conclusions.

We can also speculate how the 3D/2D transition would depend on magnetic field strength. Since $f = 1/N^2$ in our simulations, decreasing the array size may be comparable to decreasing the field strength. Our simulations at different N , combined with the above arguments, suggest that α_c increases with increasing f – that is, that flux lines are more easily broken in high flux density superconductors. Hence, for a given weak interlayer coupling, there may be an upper limiting field, above which there are no 3D flux lines at all, but only 2D pancake vortices. Such an upper limit may have been observed in experiments [7] and has been predicted theoretically [5,8].

IV. TIME-DEPENDENT BEHAVIOR

Fig. 4(a) shows both $V_p(t)$ and $V_s(t)$ for $N = 10$, $I = 0.2I_c$, and $\alpha = 0$. For this case, we find that the primary vortex moves across the array in the 5th row, while the secondary vortex remains fixed in the plaquette (10, 5). Correspondingly, $\langle V_p \rangle \neq 0$ but $\langle V_s \rangle = 0$. (Similar results are found for larger arrays.) The peaks in $V_p(t)$ correspond to the translation of the primary vortex by one plaquette. The corresponding peaks in $V_s(t)$, resulting from the weak resistive coupling between the layers, correspond to oscillations of the secondary vortex around an equilibrium position. Since the interlayer resistive coupling is very weak, there is a constant time interval between consecutive peaks in $V_p(t)$, implying that the velocity of the primary vortex does not depend on its proximity to the secondary vortex, and suggesting that the intervortex interaction nearly vanishes under these conditions. The time interval T between peaks satisfies the Josephson relation $\langle V \rangle = \frac{\hbar}{2e} \frac{2\pi}{NT}$, where $\langle V_p \rangle$ is the time-averaged voltage difference across the primary layer. This is consistent with the picture of a vortex circling the array once in an interval NT .

Fig. 4(b) shows the corresponding voltages at $N = 10$, $I = 0.16I_c$, and $\alpha = 0.01$. In this case, the primary vortex is depinned, traveling in the 5th row of the array, while the secondary vortex remains fixed in plaquette (10, 5), as in the $\alpha = 0$ case. Once again, both $V_p(t)$ and $V_s(t)$ exhibit many peaks, with the same interpretation as in 4(a). But now the interval between peaks on $V_p(t)$ is variable, implying a plaquette-dependent primary vortex velocity. The interval is smallest, and the average vortex velocity greatest, when primary and secondary vortices interval are directly superposed, and the mutual attraction is strongest. Because of the periodic boundary conditions, $V_p(t)$ is periodic, with N peaks in each period. The peak structure in $V_p(t)$ proves that an attractive interaction between vortices can be produced by interlayer Josephson coupling alone.

Fig. 5 shows $V(t)$ and the vortex paths for $N = 10$, $f = 0.01$, $\alpha = 0.04$, and $I = 0.18I_c$. In this case, the two pancake vortices form a single flux line which moves as a unit at low bias current. Both $V_p(t)$ and $V_s(t)$ are characterized by periodic double-peaked structure

[cf. Fig. 5(a)], which can be understood from the vortex spatial path shown in Fig. 5(b). The larger peaks of $V_p(t)$ and the smaller peaks of $V_s(t)$ correspond to the translation of the primary vortex by one plaquette, while the other peaks arise from the translation of the secondary vortex. $V_p(t)$ and $V_s(t)$ have the same frequency. Although the two vortices move as a unit, the vortex line is at an angle to the c axis: the primary vortex leads the secondary vortex on average by about half a plaquette. In simulations at $N = 19$, we have found that the primary vortex can lead the secondary vortex by as much as two plaquettes. As α increases, this horizontal distance decreases, showing that the interlayer vortex interaction is increasing.

Note also that $V_p(t)$ and $V_s(t)$ have slightly different waveforms, although they have the same frequency. This means that the flux line formed by the two pancakes is not rigid. Our picture is that the flux line moves as a unit across the array in a periodic motion, but that the two constituent pancakes may oscillate around their steady state positions on the flux line. The period of such an oscillation would equal that of the flux line motion.

At $I = 0.36I_c$, for this coupling, the flux line breaks into independent primary and secondary pancakes. Above this current, $\langle V_p \rangle > \langle V_s \rangle$, indicating that the primary vortex moves faster than the secondary one. Such a critical vortex velocity for flux line breaking, i. e., a 3D to 2D crossover, has been reported in high- T_c superconductors [11].

V. DISCUSSION AND CONCLUSIONS

We have studied the dynamical response of two-layer Josephson arrays to a bias current applied in the flux transformer geometry. Although this model is far from a realistic high- T_c superconductor, our numerical results agree qualitatively with some experimental studies on such materials. Thus, they may be useful in constructing more realistic models for the dynamics of high- T_c materials in this geometry.

Our results show that interlayer Josephson coupling alone is enough to bind pancake vortices into vortex lines. These lines move as a unit under the drive of an external bias

current, but may break up into 2D pancake vortices and move independently at high enough currents, provided the magnetic field is not too small. Our calculations also suggest that, for any given current, there may exist an upper magnetic field limit above which 3D flux lines are unstable in the flux transformer geometry.

Our results suggest several areas for future work. First, it would be of interest to extend this work to larger magnetic fields and finite temperatures (included via Langevin noise), in order to study the 3D-2D transition at finite fields and temperatures. Likewise, the inclusion of a finite inductive coupling between plaquettes [19,20] might lead to novel behavior not seen in the present, low-screening limit. Finally, the predicted effects might be sought experimentally, not only in high- T_c materials, but directly in two-layer Josephson arrays which could be made in the geometries described here.

VI. ACKNOWLEDGEMENTS.

We thank Prof. S. M. Girvin and Dr. Saad Hebboul for drawing this problem to our attention, and Dr. Y. M. Wan for valuable conversations. This work was supported by NSF grants DMR 90-20994 and DMR94-02131, and by the Midwest Superconductivity Consortium at Purdue University through D. O. E. Grant DE-FG90-02-ER-45427. Calculations were carried out, in part, on the CRAY Y-MP 8/864 of the Ohio Supercomputer Center.

REFERENCES

- [1] I. Giaever, Phys. Rev. Lett. **15**, 825 (1965).
- [2] J. W. Ekin and J. R. Clem, Phys. Rev. B **12**, 1753 (1975).
- [3] J. R. Clem, Phys. Rev. B **43**, 7837 (1991).
- [4] H. Safar, E. Rodriguez, F. de la Cruz, P. L. Gammel, L. F. Schneemeyer and D. J. Bishop, Phys. Rev. B **46**, 14238 (1992).
- [5] M. P. A. Fisher, Phys. Rev. Lett. **62**, 1415 (1989); D. S. Fisher, M. P. A. Fisher and D. Huse, Phys. Rev. B **43**, 130 (1991).
- [6] For a general review, see D. R. Nelson, in *Phenomenology and Applications of High-Temperature Superconductors*, edited by K. S. Bedell, M. Inui, D. Meltzer, J. R. Schrieffer, and S. Doniach, (Addison-Wesley, 1991), pp. 187-239.
- [7] W. R. White, A. Kapitulnik and M. R. Beasley, Phys. Rev. Lett. **66**, 2826 (1991).
- [8] L. I. Glazman and A. E. Koshelev, Phys. Rev. B **43**, 2835 (1991).
- [9] Y. M. Wan, S. E. Hebboul, D. C. Harris and J. C. Garland, Phys. Rev. Lett. **71**, 157 (1993); Y. M. Wan, S. E. Hebboul and J. C. Garland, Phys. Rev. Lett. **72**, 3867 (1994).
- [10] D. López, G. Nieva and F. de la Cruz, submitted to Phys. Rev. Lett. (1993).
- [11] F. de la Cruz, D. López and G. Nieva, preprint.
- [12] Y. Li and S. Teitel, Phys. Rev. Lett. **66**, 3301 (1991).
- [13] K. H. Lee, D. Stroud and S. M. Girvin, Phys. Rev. B **48**, 1233 (1993).
- [14] J. M. Duan, Phys. Rev. Lett. **70**, 3991 (1993).
- [15] Wenbin Yu, K. H. Lee and D. Stroud, Phys. Rev. B **47**, 5906 (1993).
- [16] C. J. Lobb, D. W. Abraham and M. Tinkham, Phys. Rev. B **27**, 150 (1983).

- [17] M. S. Rzchowski, S. P. Benz, M. Tinkham and C. J. Lobb, Phys. Rev. B **42**, 2041 (1990).
- [18] This would require that a vortex line would remain bound for arbitrarily large horizontal distance between pancakes on adjacent layers. Such a possibility would be reasonable if the attractive force between such pancakes were independent of separation, as is believed to be true for Josephson-coupled pancakes. (See, for example, [14], or S. Ryu *et al*, Phys.,. Rev. Lett. **68**, 710 (1992)).
- [19] D. Domínguez and J. José, Phys. Rev. Lett. **69**, 514 (1992).
- [20] H. S. J. van der Zant, T. P. Orlando, S. Watanabe, and S. Strogatz, submitted to Phys. Rev. Lett. (1994).

FIGURE CAPTIONS

1. Schematic diagram of a $2 \times 5 \times 5$ ($N = 5$) two-layer Josephson junction array. Each intersection denotes a superconducting grain. Each grain is coupled to its four intralayer neighbors, and to the nearest grain in the adjacent layer, by a resistively shunted Josephson junction (RSJ). An external magnetic field \mathbf{B} is applied perpendicular to the layers in the z direction. A bias current I is injected into each grain at one edge of the upper layer (the “primary layer”), and extracted at the opposite edge in the y direction. V_p and V_s denote the voltage drops across the primary and secondary layers (averaged over x), as shown. There are periodic boundary conditions in the x direction.
2. $I - \langle V \rangle$ characteristics for an $N = 10$ at $f = 0.01$, and three different values of α . In each case, the two curves denote V_p and V_s . (a) $\alpha = 0$; (b) $\alpha = 0.01$; (c) $\alpha = 0.04$.
3. Schematic view of the array, viewed along the x direction, and showing the current direction in junctions parallel to y axis in an $N = 11$ array. Arrows denote the direction of current flow; crosses denote the vortex pancake positions.
4. $V_p(t)$ (full curves) and $V_s(t)$ (dotted curves) in $N = 10$ arrays at $f = 0.01$ for two coupling ratios and bias currents as indicated.
5. Time-dependent voltage traces and vortex path for an $N = 10$ two-layer array at $f = 0.01$, $\alpha = 0.04$, and $I = 0.18I_c$. In both cases, the full curve corresponds to the primary vortex; the dotted curve, to the secondary vortex. (a) Voltage traces $V_p(t)$ and $V_s(t)$. (b) Schematic of time-dependent vortex position (x is the x-coordinate of vortex position; a is the lattice constant).

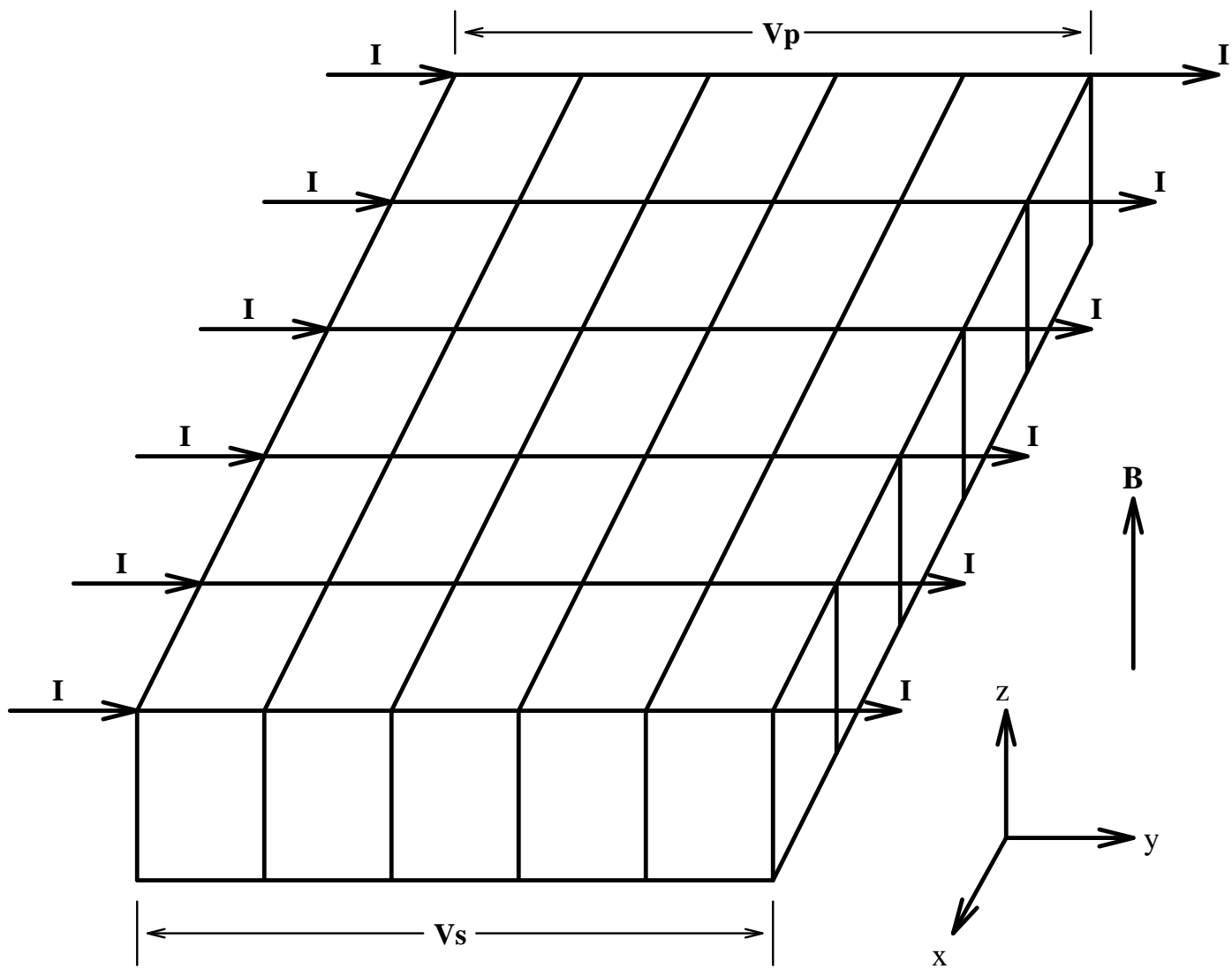


Fig. 1

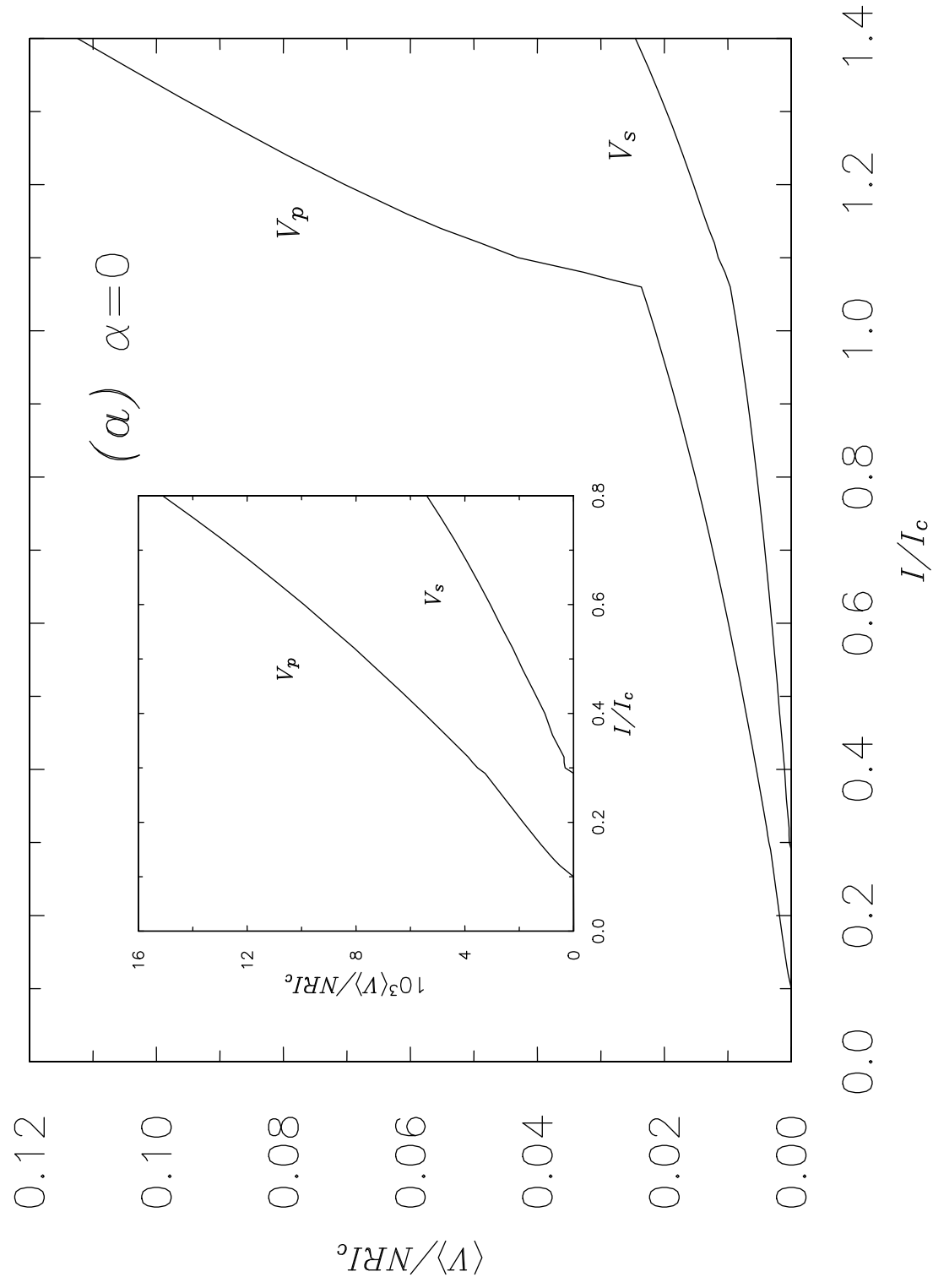


Fig. 2 (a)

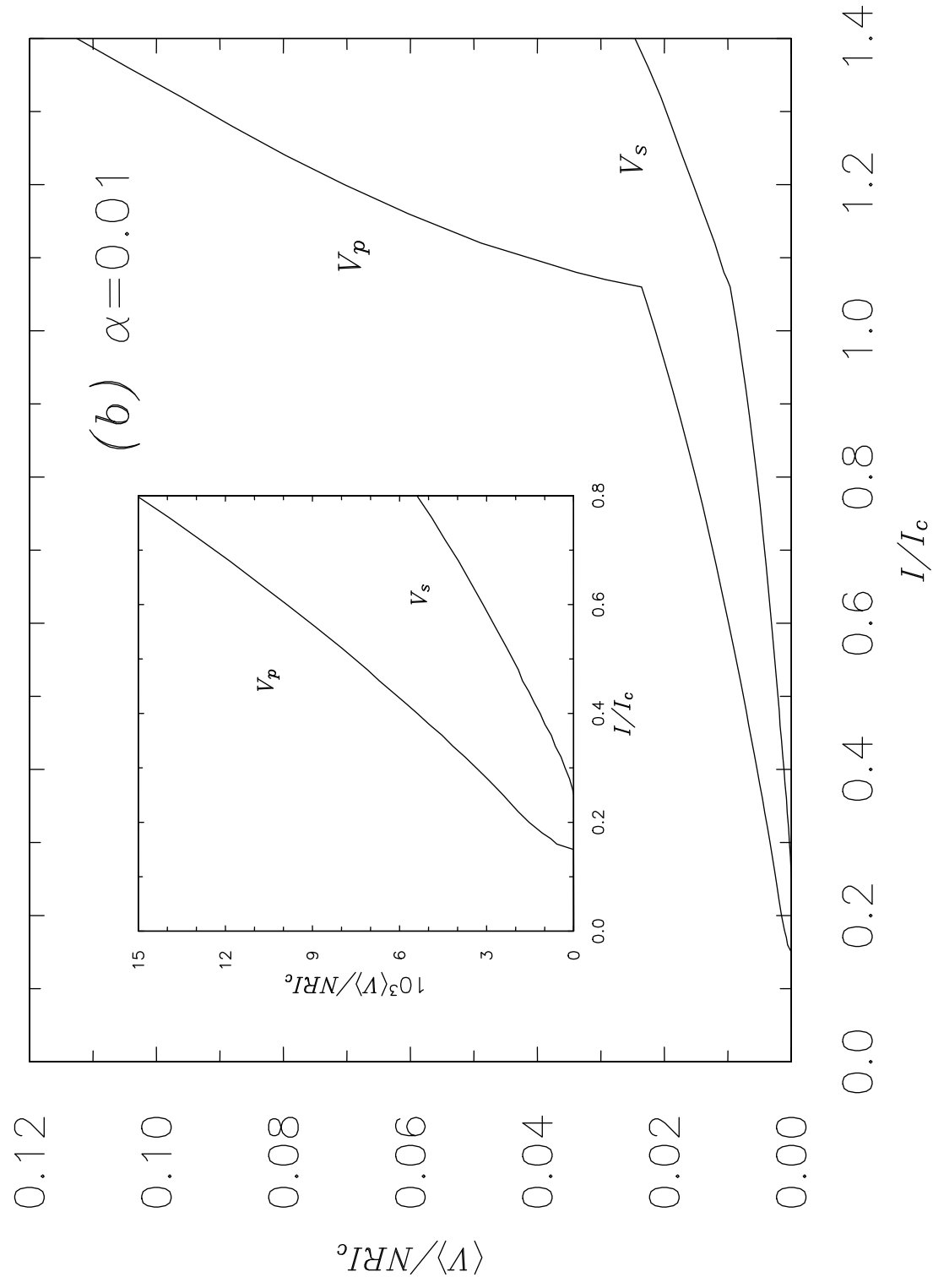


Fig. 2 (b)

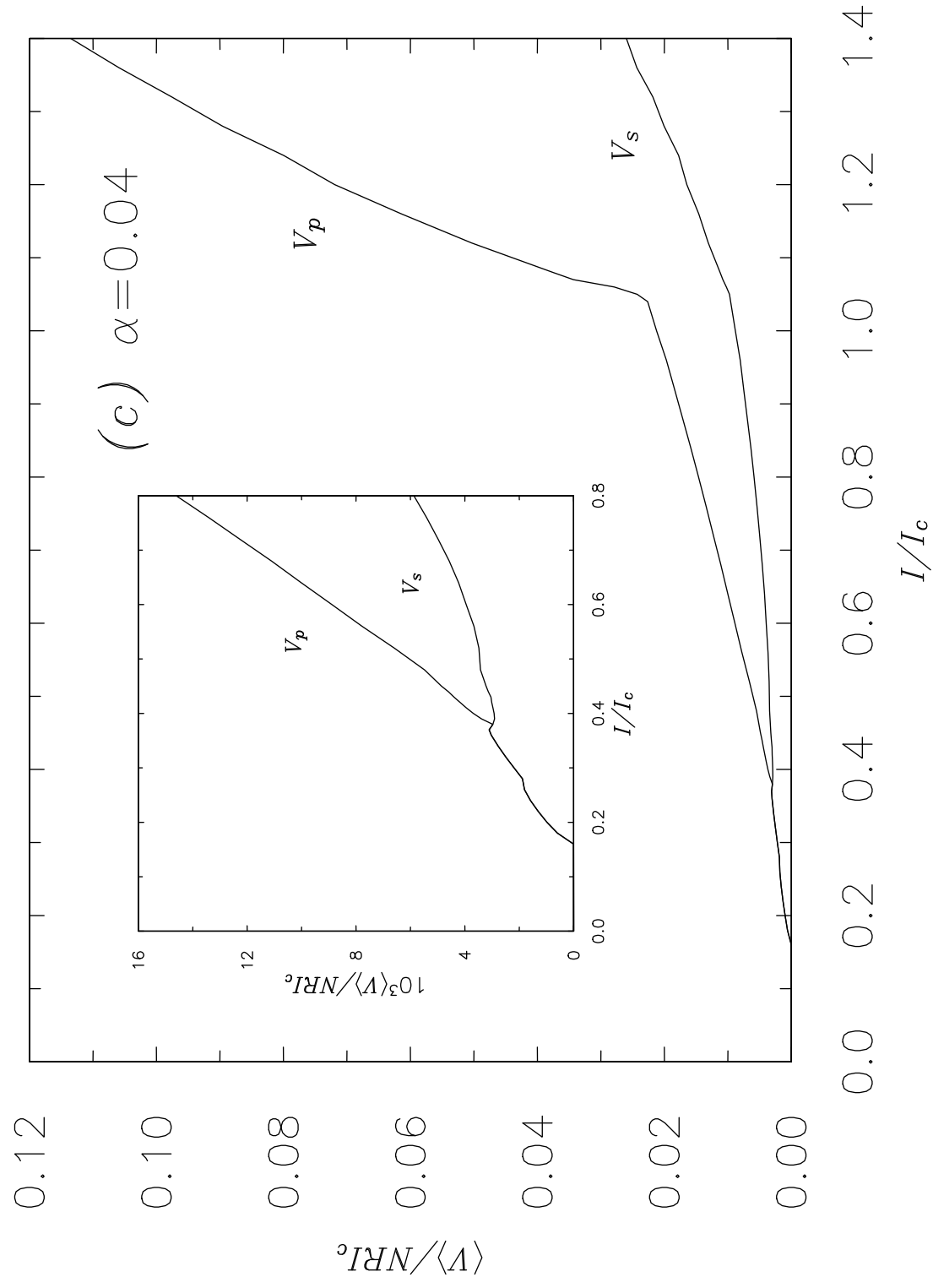


Fig. 2 (c)

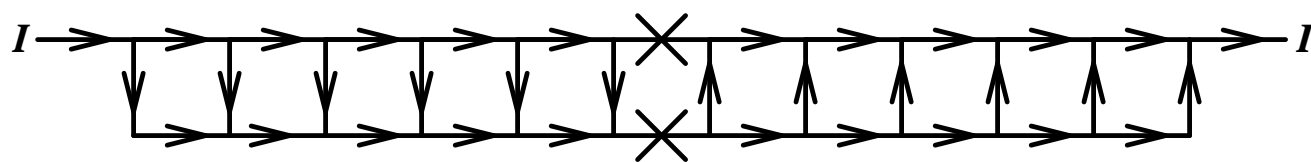


Fig. 3

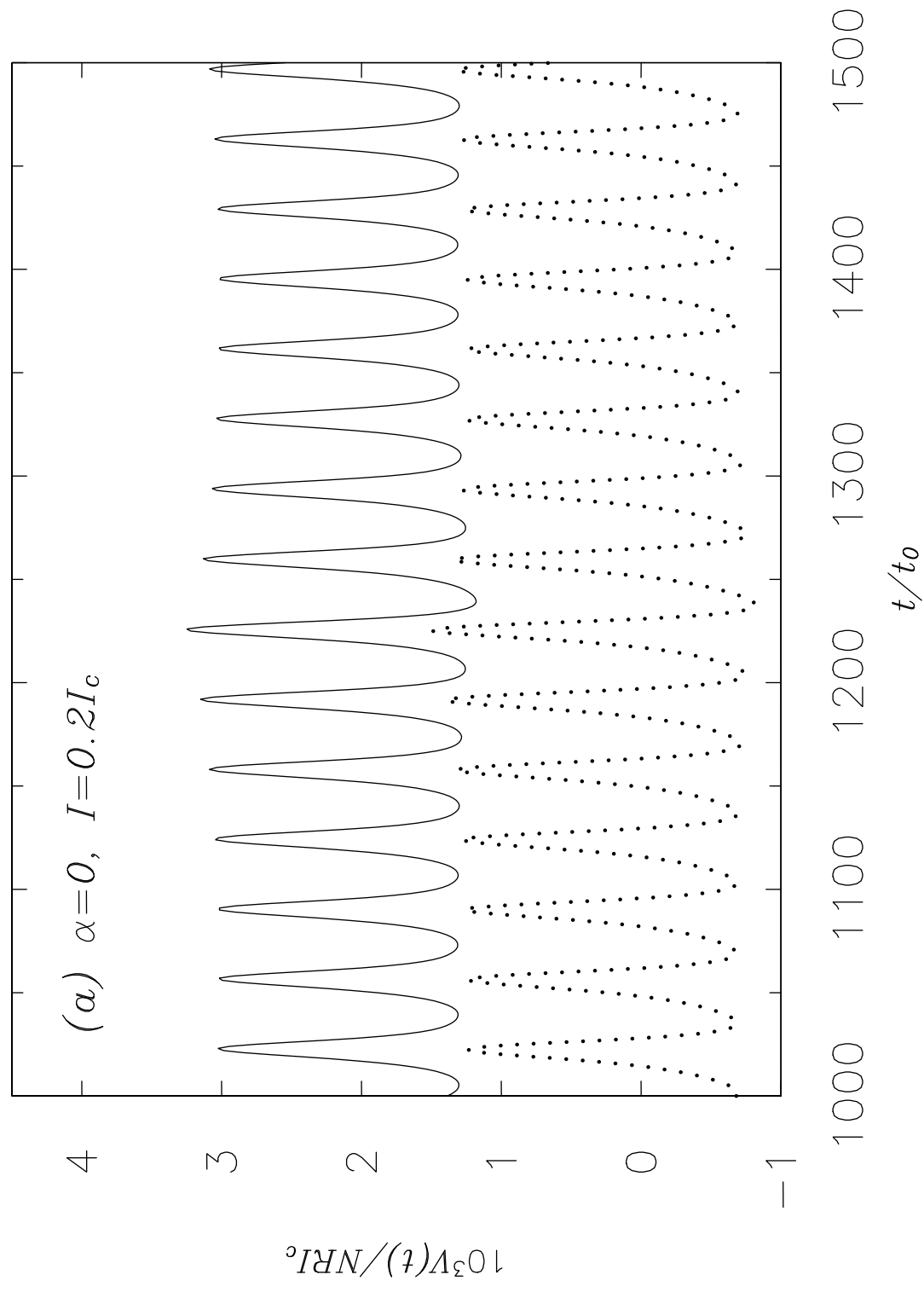


Fig. 4 (a)

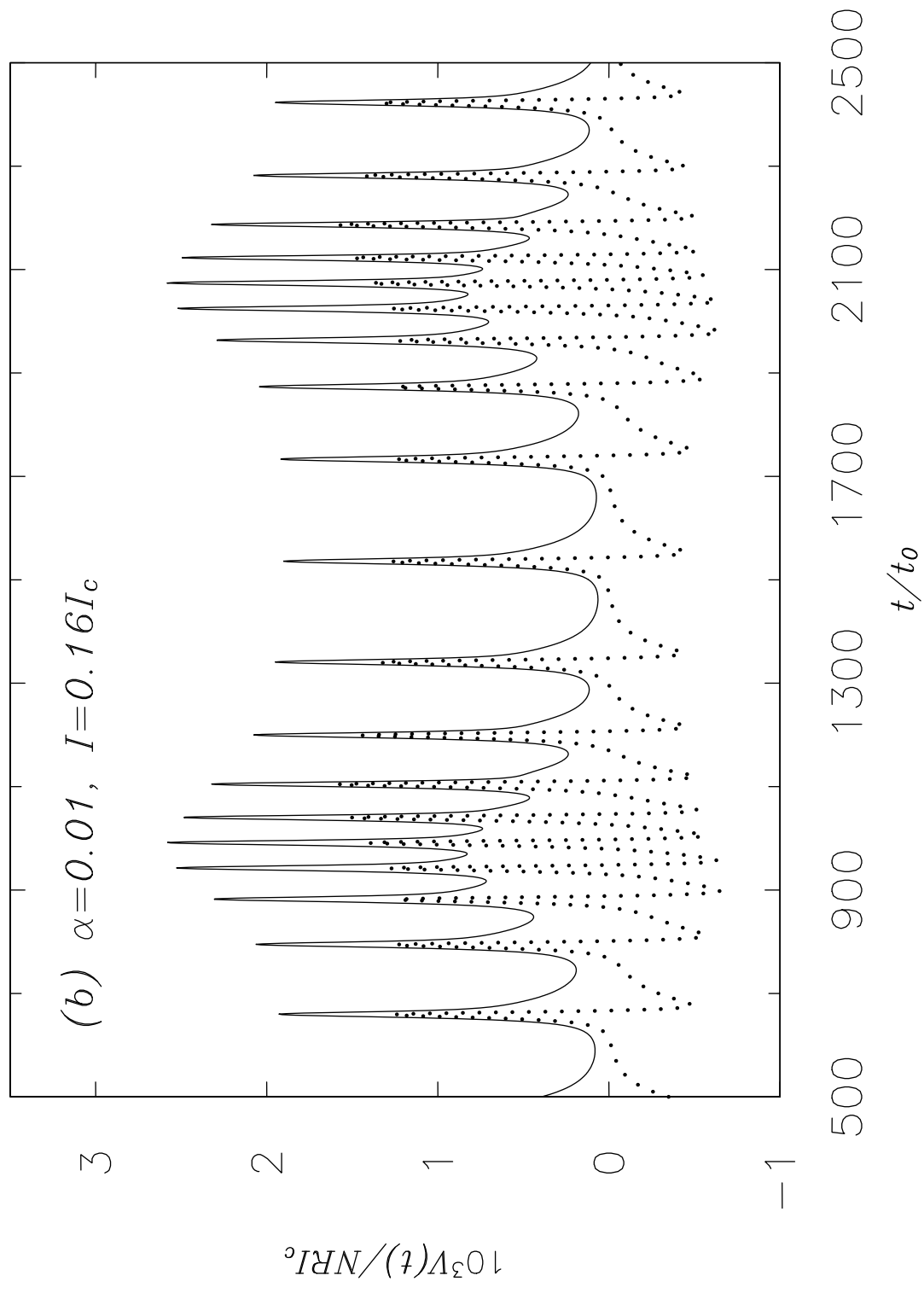


Fig. 4 (b)

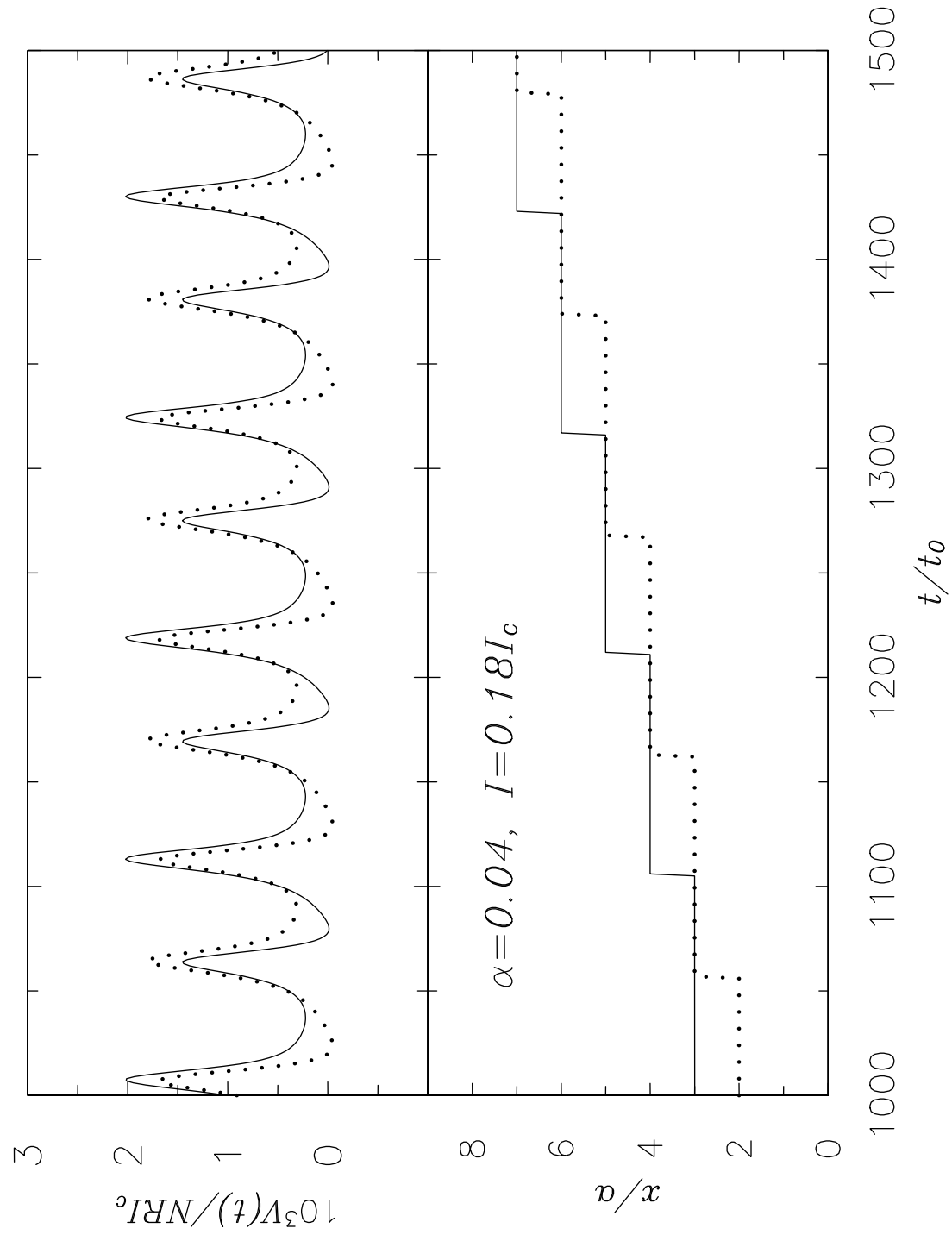


Fig. 5